Comparison and Practical Aspects of Two Approaches for Online Load Reconstruction

Y. NIU and C.-P. FRITZEN

ABSTRACT

The load reconstruction process is actually to solve an ill-posed inverse problem in structural dynamics. The recursive three-step filter (RTSF) and the Kalman filter with unknown inputs (KF-UI), two algorithms recently proposed in electrical engineering, both can simultaneously deliver the optimal estimates of the system states and the unknown inputs, without any assumption on the input dynamics. This unknown input estimation ability and the inherent real-time operation possibility make these two types of estimators very promising for online load reconstruction.

In this paper, both the RTSF and the KF-UI are first generalized to be compatible with the case that the process noise and the measurement noise are correlated. Then the reconstruction performance of the generalized RTSF (G-RTSF) and the generalized KF-UI (G-KF-UI) are evaluated using both simulations and experiments.

INTRODUCTION

The knowledge of external load applied on a structure is very important in many fields. For example, the actual loading information can help to improve the product design; the external load could be used for feed-forward control in structural vibration control design; the loading history can also be used in the damage prognosis study to predict the remaining lifetime of the investigated structure [1]. In practice, the structural loads may not be measured directly. For such a case, a widely used strategy is to reconstruct such loads from dynamic response measurements. This is often an ill-posed inverse problem, in the sense that small changes in the measurements, e.g. the existence of measurement noise, may lead to a big deviation in the reconstruction result [2].

Yan Niu and Claus-Peter Fritzen, Institute of Mechanics and Control Engineering - Mechatronics, Center for Sensor Systems (ZESS), University of Siegen, Paul-Bonatz-Strasse 9-11, Siegen 57076, Germany.

In order to solve this ill-posed inverse problem, several unknown input estimation algorithms, which can run in real-time and are robust to the measurement noise and the modelling error, have been adopted and made on-line force reconstruction become possible. Similar to the idea in [3], Niu *et al.* adopted the recently published Kalman filter with unknown inputs (KF-UI) method for the force reconstruction purpose [4]. This KF-UI method has no assumption on the input dynamics and can provide the unique least-squares and minimum-variance unbiased estimates of the system states and unknown inputs [5].

It can be proved that the KF-UI has the same filter form as the recursive three-step filter (RTSF) presented earlier by Gillijns and De Moor [6]. However, the KF-UI and the RTSF have different necessary and sufficient conditions (NASCs), which may lead to distinct requirements in the practical load reconstruction, e.g. different sensor numbers, sensor types and the need of unbiased estimate of initial condition. Furthermore, it was noticed by the authors that the employment of accelerometers will result in the correlation of the process noise and the measurement noise, which is in contradiction with the assumption made in the derivation of the KF-UI and the RTSF that the process noise and the measurement noise are uncorrelated. Such a contradiction in turn may theoretically affect the optimality of the estimation result. Motivated by this point, the RTSF and the KF-UI are first generalized to be compatible with the correlation of the process noise and the measurement noise in this paper. On the other side, the process noise is usually not so large in practice. So it is also reasonable to propose the question that how much improvement such a generalization operation can bring. To investigate the above issues, the reconstruction performance of the generalized RTSF (G-RTSF) and the generalized KF-UI (G-KF-UI) are evaluated using both simulations and experiments based on a laboratory two-storey structure.

COMMON FILTER FORM OF THE RTSF AND THE KF-UI

Consider the following linear discrete-time system,

$$\begin{aligned} \boldsymbol{x}_{k+1} &= \boldsymbol{A}_k \boldsymbol{x}_k + \boldsymbol{G}_k \boldsymbol{d}_k + \boldsymbol{w}_k \\ \boldsymbol{y}_k &= \boldsymbol{C}_k \boldsymbol{x}_k + \boldsymbol{H}_k \boldsymbol{d}_k + \boldsymbol{v}_k \end{aligned}, \tag{1}$$

where $\boldsymbol{x}_k \in R^n$ is the state vector, $\boldsymbol{d}_k \in R^m$ is the unknown input vector, and $\boldsymbol{y}_k \in R^p$ represents the output vector. $\boldsymbol{w}_k \in R^n$ is the process noise and $\boldsymbol{v}_k \in R^p$ denotes the measurement noise. Both $\boldsymbol{w}_k$ and $\boldsymbol{v}_k$ are assumed as mutually uncorrelated zero-mean and white random signals with known covariance $\boldsymbol{Q}_k = E\left[\boldsymbol{w}_k \boldsymbol{w}_k^T\right] \geq \boldsymbol{0}$ and $\boldsymbol{R}_k = E\left[\boldsymbol{v}_k \boldsymbol{v}_k^T\right] > \boldsymbol{0}$, ($E[\cdot]$ is the expectation operator). System matrices $\boldsymbol{A}_k$, $\boldsymbol{G}_k$, $\boldsymbol{C}_k$ and $\boldsymbol{H}_k$ are of appropriate dimensions, with $\boldsymbol{A}_k$ assumed to be nonsingular. Define $\hat{\boldsymbol{x}}_{k|k-1}$ as the *a priori* state estimate, $\hat{\boldsymbol{x}}_{k|k}$ the *a posteriori* state estimate, $\hat{\boldsymbol{d}}_{k|k}$ the input estimate, $\boldsymbol{P}_{k|k-1}^x$ the *a priori* state estimate error covariance, $\boldsymbol{P}_{k|k}^x$ the *a posteriori* state estimate error covariance, $\boldsymbol{P}_k^d$ the input estimate error covariance, and $\boldsymbol{P}_k^{xd}$ the cross covariance between the estimate errors of $\boldsymbol{x}_k$ and $\boldsymbol{d}_k$. It can be proved that the RTSF and the KF-UI has the following common filter form.

Initialization

$$\hat{\boldsymbol{x}}_{0|0},\ \hat{\boldsymbol{d}}_{0|0},\ \boldsymbol{P}^{x}_{0|0},\ \boldsymbol{P}^{d}_{0},\ \boldsymbol{P}^{xd}_{0}; \tag{2}$$

Time update

$$\hat{\boldsymbol{x}}_{k|k-1} = \boldsymbol{A}_{k-1}\hat{\boldsymbol{x}}_{k-1|k-1} + \boldsymbol{G}_{k-1}\hat{\boldsymbol{d}}_{k-1|k-1}; \tag{3}$$

$$\boldsymbol{P}^{x}_{k|k-1} = \begin{bmatrix}\boldsymbol{A}_{k-1} & \boldsymbol{G}_{k-1}\end{bmatrix}\begin{bmatrix}\boldsymbol{P}^{x}_{k-1|k-1} & \boldsymbol{P}^{xd}_{k-1}\\ \boldsymbol{P}^{dx}_{k-1} & \boldsymbol{P}^{d}_{k-1}\end{bmatrix}\begin{bmatrix}\boldsymbol{A}^{T}_{k-1}\\ \boldsymbol{G}^{T}_{k-1}\end{bmatrix} + \boldsymbol{Q}_{k-1}; \tag{4}$$

Measurement update

$$\widetilde{\boldsymbol{R}}_{k} = \boldsymbol{C}_{k}\boldsymbol{P}^{x}_{k|k-1}\boldsymbol{C}^{T}_{k} + \boldsymbol{R}_{k}; \tag{5}$$

$$\boldsymbol{M}_{k} = \left(\boldsymbol{H}^{T}_{k}\widetilde{\boldsymbol{R}}^{-1}_{k}\boldsymbol{H}_{k}\right)^{-1}\boldsymbol{H}^{T}_{k}\widetilde{\boldsymbol{R}}^{-1}_{k}; \tag{6}$$

$$\boldsymbol{P}^{d}_{k} = \left(\boldsymbol{H}^{T}_{k}\widetilde{\boldsymbol{R}}^{-1}_{k}\boldsymbol{H}_{k}\right)^{-1}; \tag{7}$$

$$\boldsymbol{K}_{k} = \boldsymbol{P}^{x}_{k|k-1}\boldsymbol{C}^{T}_{k}\widetilde{\boldsymbol{R}}^{-1}_{k}; \tag{8}$$

$$\boldsymbol{P}^{x}_{k|k} = \boldsymbol{P}^{x}_{k|k-1} - \boldsymbol{K}_{k}\left(\widetilde{\boldsymbol{R}}_{k} - \boldsymbol{H}_{k}\boldsymbol{P}^{d}_{k}\boldsymbol{H}^{T}_{k}\right)\boldsymbol{K}^{T}_{k}; \tag{9}$$

$$\boldsymbol{P}^{xd}_{k} = \left(\boldsymbol{P}^{dx}_{k}\right)^{T} = -\boldsymbol{K}_{k}\boldsymbol{H}_{k}\boldsymbol{P}^{d}_{k}; \tag{10}$$

$$\hat{\boldsymbol{d}}_{k|k} = \boldsymbol{M}_{k}\left(\boldsymbol{y}_{k} - \boldsymbol{C}_{k}\hat{\boldsymbol{x}}_{k|k-1}\right); \tag{11}$$

$$\hat{\boldsymbol{x}}_{k|k} = \hat{\boldsymbol{x}}_{k|k-1} + \boldsymbol{K}_{k}\left(\boldsymbol{y}_{k} - \boldsymbol{C}_{k}\hat{\boldsymbol{x}}_{k|k-1} - \boldsymbol{H}_{k}\hat{\boldsymbol{d}}_{k|k}\right). \tag{12}$$

COMMON FILTER FORM OF THE G-RTSF AND THE G-KF-UI

Define $E\left[\boldsymbol{w}_{k-1}\boldsymbol{v}^{T}_{k}\right] = \boldsymbol{S}_{k}$, the common filter form of the G-RTSF and the G-KF-UI is derived using the method suggested in [7].

Initialization

$$\hat{\boldsymbol{x}}_{0|0},\ \hat{\boldsymbol{d}}_{0|0},\ \boldsymbol{P}^{x}_{0|0},\ \boldsymbol{P}^{d}_{0},\ \boldsymbol{P}^{xd}_{0}; \tag{13}$$

Time update

$$\hat{\boldsymbol{x}}_{k|k-1} = \boldsymbol{A}_{k-1}\hat{\boldsymbol{x}}_{k-1|k-1} + \boldsymbol{G}_{k-1}\hat{\boldsymbol{d}}_{k-1|k-1}; \tag{14}$$

$$\boldsymbol{P}^{x}_{k|k-1} = \begin{bmatrix}\boldsymbol{A}_{k-1} & \boldsymbol{G}_{k-1}\end{bmatrix}\begin{bmatrix}\boldsymbol{P}^{x}_{k-1|k-1} & \boldsymbol{P}^{xd}_{k-1}\\ \boldsymbol{P}^{dx}_{k-1} & \boldsymbol{P}^{d}_{k-1}\end{bmatrix}\begin{bmatrix}\boldsymbol{A}^{T}_{k-1}\\ \boldsymbol{G}^{T}_{k-1}\end{bmatrix} + \boldsymbol{Q}_{k-1}; \tag{15}$$

Measurement update

$$\widetilde{\boldsymbol{R}}_k = \boldsymbol{C}_k \boldsymbol{P}^x_{k|k-1} \boldsymbol{C}^T_k + \boldsymbol{R}_k + \boldsymbol{C}_k \boldsymbol{S}_k + \boldsymbol{S}^T_k \boldsymbol{C}^T_k ; \tag{16}$$

$$\boldsymbol{M}_k = \left(\boldsymbol{H}^T_k \widetilde{\boldsymbol{R}}^{-1}_k \boldsymbol{H}_k\right)^{-1} \boldsymbol{H}^T_k \widetilde{\boldsymbol{R}}^{-1}_k ; \tag{17}$$

$$\boldsymbol{P}^d_k = \left(\boldsymbol{H}^T_k \widetilde{\boldsymbol{R}}^{-1}_k \boldsymbol{H}_k\right)^{-1} ; \tag{18}$$

$$\boldsymbol{K}_k = \left(\boldsymbol{P}^x_{k|k-1} \boldsymbol{C}^T_k + \boldsymbol{S}_k\right) \widetilde{\boldsymbol{R}}^{-1}_k ; \tag{19}$$

$$\boldsymbol{P}^x_{k|k} = \boldsymbol{P}^x_{k|k-1} - \boldsymbol{K}_k \left(\widetilde{\boldsymbol{R}}_k - \boldsymbol{H}_k \boldsymbol{P}^d_k \boldsymbol{H}^T_k\right) \boldsymbol{K}^T_k ; \tag{20}$$

$$\boldsymbol{P}^{xd}_k = \left(\boldsymbol{P}^{dx}_k\right)^T = -\boldsymbol{K}_k \boldsymbol{H}_k \boldsymbol{P}^d_k ; \tag{21}$$

$$\hat{\boldsymbol{d}}_{k|k} = \boldsymbol{M}_k \left(\boldsymbol{y}_k - \boldsymbol{C}_k \hat{\boldsymbol{x}}_{k|k-1}\right); \tag{22}$$

$$\hat{\boldsymbol{x}}_{k|k} = \hat{\boldsymbol{x}}_{k|k-1} + \boldsymbol{K}_k \left(\boldsymbol{y}_k - \boldsymbol{C}_k \hat{\boldsymbol{x}}_{k|k-1} - \boldsymbol{H}_k \hat{\boldsymbol{d}}_{k|k}\right). \tag{23}$$

The NASCs of the G-RTSF and the G-KF-UI are listed in *Table 1*. It is noted here that the G-RTSF has the same NASCs as those of the RTSF, and the G-KF-UI has the same NASCs as those of the KF-UI.

***Table 1.** Necessary And Sufficient Conditions (NASCs)*

RTSF / G-RTSF	KF-UI / G-KF-UI
a) Unbiased estimate $\hat{\boldsymbol{x}}_0$ of $\boldsymbol{x}_0$ is available; b) $\boldsymbol{H}_k$ has full column rank, $(k \geq 1)$.	a) $p \geq n/2 + m$; b) $\left[\boldsymbol{C}^T_0, \ \ \boldsymbol{A}^T_0 \boldsymbol{C}^T_1, \ \ \ldots \ \ , \boldsymbol{A}^T_0 \boldsymbol{A}^T_1 \cdots \boldsymbol{A}^T_{k-1} \boldsymbol{C}^T_k\right]^T$ has full column rank, $(k \geq 1)$; c) $\left[\boldsymbol{H}_i - \boldsymbol{C}_i \boldsymbol{A}^{-1}_i \boldsymbol{G}_i\right]$ has full column rank, $(i = 0,1,2,\cdots,k-1; k \geq 1)$; d) $\boldsymbol{H}_k$ has full column rank, $(k \geq 1)$.

Either from an experimental modal analysis or from an updated computational model (e.g. finite element model), a structure can be represented in the form of Eq. (1) by defining the state vector as $\boldsymbol{x}_k = \left[\boldsymbol{q}^T_k; \ \ \dot{\boldsymbol{q}}^T_k\right]^T$, where $\boldsymbol{q}_k \in R^{n/2}$ represents the modal displacement vector and $\dot{\boldsymbol{q}}_k \in R^{n/2}$ denotes the modal velocity vector. Then the NASC (a) of the G-RTSF requires that the unbiased estimate of the initial modal displacement and the initial modal velocity should be known. According to the analysis in [4], the NASC (b) of the G-RTSF and the NASC (d) of the G-KF-UI indicate the number of acceleration measurements should be at least equal to the number of unknown input forces. The NASC (a) of the G-KF-UI requires the sensor number should be at least equal to the sum of the number of unknown input forces and the number of modes included in the structural model. The NASC (b) and (c) of the G-KF-UI restrict the sensor number, sensor types and sensor locations. From the analysis above, it seems that the G-RTSF may need less sensors (i.e. only accelerometers are needed by the G-RTSF) when the unbiased estimate of the initial condition is available.

RECONSTRUCTION PERFORMANCE EVALUATION

In this section, a laboratory two-storey structure is selected as a benchmark. Using the PolyMAX algorithm implemented in the commercial software *LMS Test.Lab*, the modal model of this structure was identified in which the first two modes in the x direction are included. The identified modal model was transformed to the form as in Eq. (1). According to the NASCs listed in *Table 1*, the G-RTSF needs only two accelerometers, while the G-KF-UI needs not only two accelerometers but also two strain gauges. The process noise and the measurement noise are both assumed to be stationary, and their covariance matrices are named as $\boldsymbol{Q}$ and $\boldsymbol{R}$. According to the real measurements from the sensors in the laboratory condition, the variance of the noise from the strain gauge was set as $1\times10^{-13}\, m^2/m^2$ and the variance of the noise from the accelerometer was chosen as $0.5\times10^{-2}\, m^2/s^4$. The diagonal elements of $\boldsymbol{Q}$ are selected as 0, 0, 1×10^{-3} and 1×10^{-3}, respectively, and the off diagonal elements are all set as 0. The identified structural model and the settings for the process noise and the measurement noise are used in the following simulation and experimental studies.

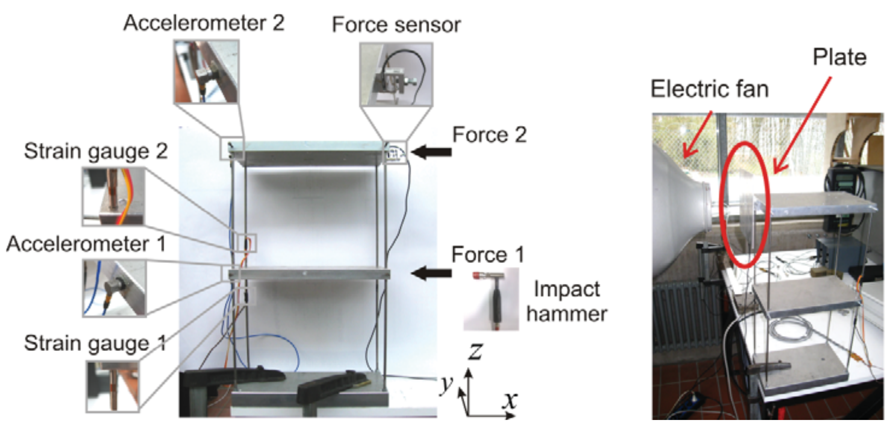

Figure 1. *Laboratory Two-Storey Structure: under impact force (left); under wind load (right)*

Simulation Study

As previously mentioned in the introduction section, one of the motivations of this paper is to investigate how much improvement the G-KF-UI and the G-RTSF can bring compared to the KF-UI and the RTSF. This issue was study in this subsection by using a simulation. The two input forces were both set as 0. The identified structural model was used as the system model. The process noise and the measurement noise were simulated as normally distributed zero-mean white random signals, with variance values set in $\boldsymbol{Q}$ and $\boldsymbol{R}$. This simulation was performed in the MATLAB SIMULINK environment and the simulation time was 120 seconds. Part of the reconstructed *Force*

1 and *Force 2* is shown in *Figure 2*, and the variances of the reconstruction errors are listed in *Table 2*. It can be seen that the variances of the reconstruction errors from the G-KF-UI and the G-RTSF are almost equal to those from the KF-UI and the RTSF for this case. Only very small improvements are brought. This is also reflected in *Figure 2*, where the red curves and the blue curves are almost superimposed. Besides this, it is also noticed that the reconstructed forces from the RTSF and the G-RTSF drift away from their real values. In order to investigate the reasons for such a drifting, more simulation and experimental studies are carried out in the subsequent subsection.

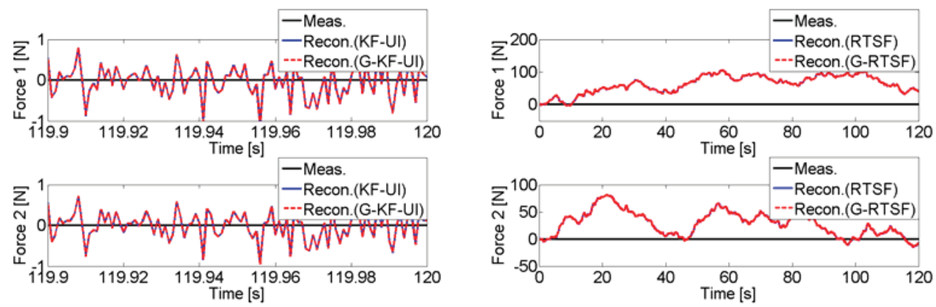

Figure 2. *Reconstruction Result: from the KF-UI and the G-KF-UI (left); from the RTSF and the G-RTSF (right)*

Table 2. *Variance of the Reconstruction Error*

Method	Variance [N^2] of	
	Recon. Error of Force 1	*Recon. Error of Force 2*
KF-UI	0.12120581	0.09353909
G-KF-UI	0.12119934	0.09352850
RTSF	$7.2250781\ 1\times10^{2}$	$5.14929214\ \times10^{2}$
G-RTSF	7.22507650×10^{2}	5.14929354×10^{2}

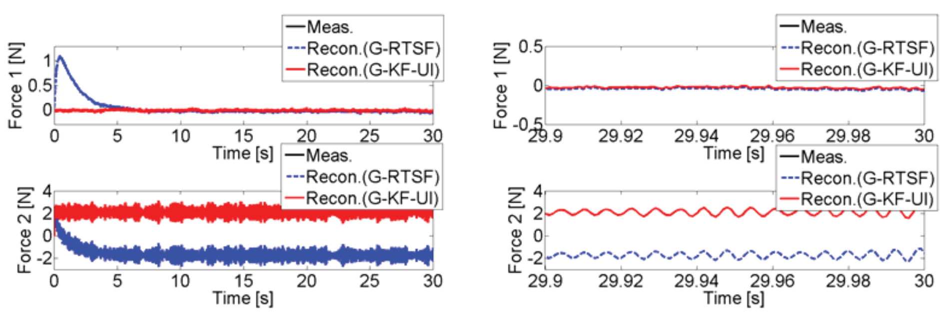

Figure 3. *Reconstructed Wind Load in the Simulation Study with Biased Estimate of the Initial Condition: the whole duration (left); the enlarged plot (right)*

Another interesting point is how the reconstruction performance will be when the estimate of the initial condition is biased. Because in some practical cases (e.g. wind load), it is not so easy to get the unbiased estimate of the initial condition. In this study, the wind load was generated by an electric fan and applied on the upper storey of the two-storey structure, where a plate was attached to collect the wind load, as shown in

Figure 1. A force sensor was placed between the plate and the upper storey to measure the wind load. The measured wind load was fed into the structural model as input force, and the generated structural responses from the structural model were provided to the G-KF-UI and the G-RTSF for reconstructing this wind load. In this procedure, no process noise and no measurement noise were considered. The reconstruction results from the G-KF-UI and the G-RTSF are shown in *Figure 3*. It can be seen that a deviation appears in the reconstruction result of the G-RTSF, while the G-KF-UI still can reconstruct the forces. This actually shows the ability of the strain gauges in measuring the static part of the input force and correcting the biased estimate of the initial condition.

Experimental Study

After an evaluation study in the simulation environment, real structural response measurements are used in the experimental study, where an impact force and a wind load were applied. As shown in *Figure 4* and *Figure 5*, the G-KF-UI still can reconstruct both types of forces, while the reconstructed forces from the G-RTSF drift away from their real values again. One explanation to this is that there is a slowly changing bias existing in the acceleration measurement, as shown in *Figure 6*. Such bias may let the G-RTSF "think" that there is a "force" applied on the structure. Besides this, it is also found that the poles of the discrete-time structural model are quite close to the unit circle, which indicates the system is quite sensitive to the noise. The employment of strain gauges somehow makes the G-KF-UI more robust to the noise. Furthermore, even though the reconstructed forces from the G-RTSF drift way, the acceleration measurements were still successfully reconstructed by these two approaches for the wind load case, as shown in *Figure 7*. This is due to the inter connection of the state estimate and input estimate of the G-KF-UI and the G-RTSF. Such acceleration measurement reconstruction ability was also presented in [8].

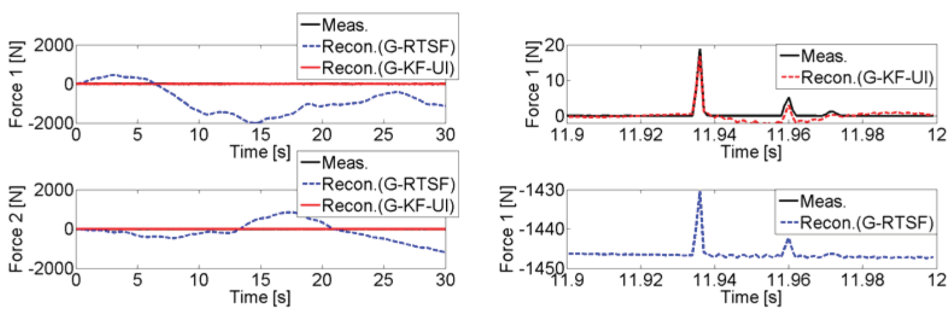

Figure 4. *Reconstructed Impact Force in the Experimental Study: the whole duration (left); the enlarged plot (right)*

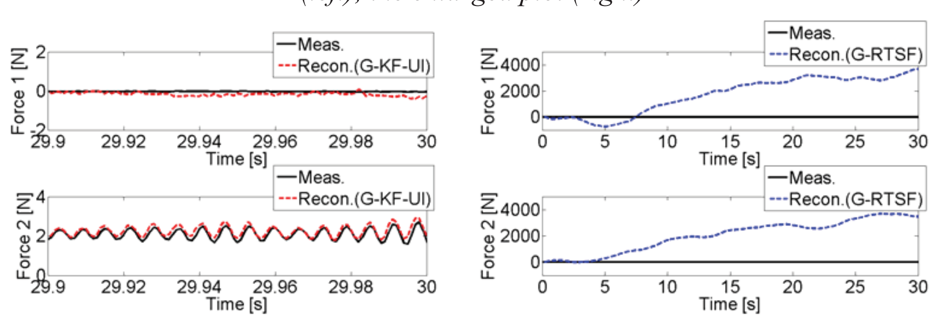

Figure 5. *Reconstructed Wind Load in the Experimental Study*

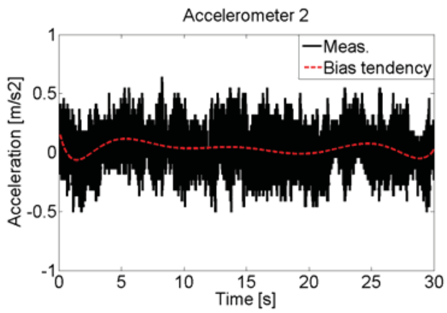

Figure 6. Slowly Changing Bias in the Measurement from Accelerometer 2

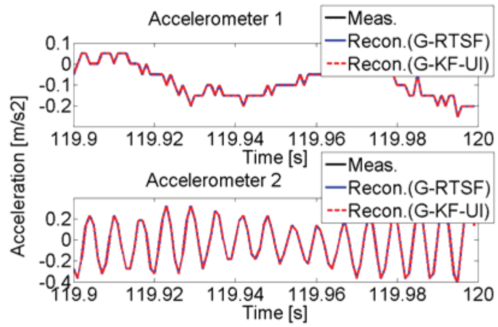

Figure 7. Reconstructed Acceleration Measurements in the Experimental Study

CONCLUSIONS

According to the analysis in this paper, when the process noise is small, the complexity of considering the correlation of the process noise and the measurement noise can be ignored and the KF-UI can be directly used for force reconstruction instead of the G-KF-UI. It is possible to use either the RTSF or the G-RTSF to reconstruct the peak value of the impact forces with only accelerometers, but these two methods are very sensitive to the measurement noise. The KF-UI and the G-KF-UI can reconstruct both impact force and the wind load with biased estimate of the initial condition, but both acceleration and strain (or displacement) measurements are needed.

ACKNOWLEDGEMENT

The authors are grateful to the Research School on Multi-Modal Sensor Systems for Environmental Exploration (MOSES) program and the Center for Sensor Systems (ZESS) for the support to this research work.

REFERENCES

1. Mueller, I., Larrosa, C., Roy, S. and Chang, F.-K. 2009. "An Integrated Diagnostic and Prognostic SHM Technology for Structural Health Management", in *Proceedings of IWSHM 2009,* September 9-11, Stanford, CA, USA, pp. 399 - 409.
2. Stevens, K.K. 1987. "Force Identification Problems - An Overview", in *Spring Meeting of SEM*, pp. 838 - 844.
3. Hwang, J.-S., Kareem, A. and Kim, W.J. 2009. "Estimation of Modal Loads using Structural Response", *Journal of Sound and Vibration,* 326, pp. 522 - 539.
4. Niu, Y., Klinkov, M. and Fritzen, C.-P. 2011. "Online Force Reconstruction using An Unknown-Input Kalman Filter Approach", in *Proceedings of EURODYN 2011*, July 4 - 6, Leuven, Belgium, pp. 2569-2576.
5. Pan, S., Su, H., Wang, H. and Chu, J. 2011. "The Study of Joint Input and State Estimation with Kalman Filtering", *Transactions of the Institute of Measurement and Control*, 33(8), pp. 901-918.
6. Gillijns, S. and De Moor, B. 2007. "Unbiased Minimum-Variance Input and State Estimation for Linear Discrete-Time Systems with Direct Feedthrough", *Automatica*, 43, pp. 934 - 937.
7. Brown, R.G. and Hwang, P.Y.C. 1997. *Introduction to Random Signals and Applied Kalman Filtering: with MATLAB Exercises and Solutions*. John Wiley & Sons, Inc.
8. Lourens, E., Lombaert, G., Papadimitriou, C. and De Roeck, G. 2011. "Joint Input-Response Predictions in Structural Dynamics", in *Proceedings of EURODYN 2011*, July 4 - 6, Leuven, Belgium, pp. 2543 - 2548.